HDGF enhances VEGF-dependent angiogenesis and FGF-2 is a VEGF-independent angiogenic factor in non-small cell lung cancer

RYOJI EGUCHI and ICHIRO WAKABAYASHI

Department of Environmental and Preventive Medicine, Hyogo College of Medicine, Nishinomiya, Hyogo 663-8501, Japan

Abstract. Non-small cell lung cancer (NSCLC) accounts for over 80% of all diagnosed lung cancer cases. Lung cancer is the leading cause of cancer-related deaths worldwide. Most NSCLC cells overexpress vascular endothelial growth factor-A (VEGF-A) which plays a pivotal role in tumour angiogenesis. Anti-angiogenic therapies including VEGF-A neutralisation have significantly improved the response rates, progression-free survival and overall survival of patients with NSCLC. However, the median survival of these patients is shorter than 18 months, suggesting that NSCLC cells secrete VEGF-independent angiogenic factors, which remain unknown. We aimed to explore these factors in human NSCLC cell lines, A549, Lu99 and EBC-1 using serum-free culture, to which only EBC-1 cells could adapt. By mass spectrometry, we identified 1,007 proteins in the culture supernatant derived from EBC-1 cells. Among the identified proteins, interleukin-8 (IL-8), macrophage migration inhibitory factor (MIF), galectin-1, midkine (MK), IL-18, galectin-3, VEGF-A, hepatoma-derived growth factor (HDGF), osteopontin (OPN), connective tissue growth factor (CTGF) and granulin (GRN) are known to be involved in angiogenesis. Tube formation, neutralisation and RNA interference assays revealed that VEGF-A and HDGF function as angiogenic factors in EBC-1 cells. To confirm whether VEGF-A and HDGF also regulate angiogenesis in the other NSCLC cell lines, we established a novel culture method. NSCLC cells were embedded in collagen gel and cultured three-dimensionally. Tube formation, neutralisation and RNA interference assays using the three-dimensional (3D) culture supernatant showed that VEGF-A and HDGF were not angiogenic factors in Lu99 cells. By gene microarray in EBC-1 and Lu99 cells, we identified 61 mRNAs expressed only in Lu99 cells. Among these mRNAs, brain-derived neurotrophic factor (BDNF), fibroblast growth factor-2 (FGF-2) and FGF-5 are known to be involved in angiogenesis. Tube formation and neutralisation assays clarified that FGF-2 functions as an angiogenic factor in Lu99 cells. These results indicate that HDGF enhances VEGF-dependent angiogenesis and that FGF-2 is a VEGF-independent angiogenic factor in human NSCLC cells.

Correspondence to: Dr Ryoji Eguchi, Department of Environmental and Preventive Medicine, Hyogo College of Medicine, 1-1 Mukogawa-cho, Nishinomiya, Hyogo 663-8501, Japan
E-mail: r-eguchi@hyo-med.ac.jp

Introduction

Lung cancer is the leading cause of cancer-related deaths worldwide and over 80% of patients with lung cancer are diagnosed with non-small cell lung cancer (NSCLC) (1,2). Platinum-based doublets, established in a series of clinical trials as the standard treatment for NSCLC, have increased the response rates and median survival of patients with NSCLC compared with the same platinum alone (3). However, the median survival of these patients remains less than 14 months.

Tumour angiogenesis, the formation of new vasculature to supply nutrition and oxygen in a direction from pre-existing blood vessels toward tumours, is prerequisite for tumour progression (4). Most tumours, including NSCLC, associated with tumour angiogenesis overexpress vascular endothelial growth factors (VEGFs), and VEGF/VEGF receptor (VEGFR) axes, particularly the VEGF-A/VEGFR2 axis, play a pivotal role in angiogenesis (5). Binding of VEGF-A to VEGFR2 results in tyrosine phosphorylation in VEGFR2 and subsequent activation of cellular substrates including extracellular-regulated kinase 1/2 (ERK1/2), members of the mitogen-activated

protein kinase superfamily, which regulate cell proliferation, differentiation and survival (5).

Anti-angiogenic therapy targeting the VEGF-A/VEGFR2 axis is a promising strategy aimed at preventing tumour growth, invasion and metastasis (6). The addition of bevacizumab, a monoclonal antibody to VEGF-A, to the platinum-based doublets is currently used for first-line therapy for advanced and unresectable NSCLC except in the case of squamous cell carcinoma (3). Recently, the combination of docetaxel and ramucirumab, a monoclonal antibody to VEGFR2, was approved for second-line therapy for advanced and unresectable NSCLC including squamous cell carcinoma (3,7). Both anti-angiogenic therapies significantly improve the response rates, progression-free survival and overall survival of patients with NSCLC, yet the median survival of the patients was shorter than 18 months. These studies suggest that NSCLC cells secrete VEGF-independent angiogenic factors and that more effective antiangiogenic-antibody therapies are expected to be developed.

In the present study, we explored VEGF-independent angiogenic factors in NSCLC and demonstrated that hepatoma-derived growth factor (HDGF) enhances VEGF-dependent angiogenesis and that fibroblast growth factor-2 (FGF-2) is a VEGF-independent angiogenic factor in human NSCLC cells.

Materials and methods

Cell culture, morphological observation and reagents. Human NSCLC cell lines, A549, Lu99 and EBC-1, (Riken BioResearch Center, Tsukuba, Japan) were cultured in 100-mm dishes (Becton Dickinson Labware) in RPMI-1640 medium supplemented with 10% fetal bovine serum (FBS) (Moregate Biotech), penicillin (5 μg/ml), streptomycin (5 μg/ml) and neomycin (10 μg/ml). Human umbilical vein endothelial cells (HUVECs) isolated from human umbilical cord were purchased from Lonza Walkersville, Inc. and cultured as described previously (8). Incubation was carried out at 37˚C in 95% air and 5% CO_2. Phase contrast imaging with a light microscope (Nikon, Tokyo, Japan) was performed at the indicated time points. Representative images of phase contrast were obtained. Type I collagen solution (Atelocollagen Bovine Dermis, IPC-30) was purchased from Koken, Co., Ltd. Other chemicals were purchased from Sigma-Aldrich; Merck KGaA unless otherwise stated. All cells used in this study were authenticated by short tandem repeat analysis and confirmed to be mycoplasma-negative.

Serum-free culture. Serum-free culture was performed as described previously (8) with slight modifications. The NSCLC cell lines were trypsinised, spun down at 4˚C and washed twice with cold serum-free MCDB-104GK medium (Nihon Pharmaceutical Co., Ltd.). The cell lines were then serum-deprived, seeded at a density of 0.2 or $2x10^5$ cells/cm^2 in 35-mm dishes (Asahi Techno Glass), 60-mm dishes (Asahi Techno Glass) or 100-mm dishes (Becton Dickinson Labware) in serum-free MCDB-104GK medium supplemented with penicillin (5 μg/ml), streptomycin (5 μg/ml) and neomycin (10 μg/ml) and incubated for 24 h. The serum-free culture supernatant derived from EBC-1 cells (EBC-1 supernatant) and the cells were spun down, and each supernatant was filtrated

through a 0.45-μm polyvinylidene difluoride membrane filter (Merck Millipore, Italy) and concentrated by ultrafiltration (Amicon Ultra 3K, Merck Millipore). Protein concentrations in EBC-1 supernatants were determined using the Bradford method.

Flow cytometric analysis of cell death. Cell death analyses in EBC-1 cells were performed using the Muse™ Cell Analyzer (Merck Millipore) according to the manufacturer's instructions as described previously (8) with slight modifications. Briefly, EBC-1 cells were harvested after 24-h cultures with or without 10% FBS and suspended at $3x10^5$ cells/ml in phosphate-buffered saline (PBS) containing 1% FBS. Each 100-μl cell suspension was then labelled for 20 min in the dark with the same volume of Annexin-V/7-amino-actinomycin D (7-AAD) reagent (Muse™ Annexin-V & Dead Cell kit, Merck Millipore). Quantitative detection of Annexin V/7-AAD-positive cells was performed using the Muse™ Cell Analyzer.

Formation of capillary-like tube structures (tube formation) in sandwich culture and quantitative analysis. Tube formation in sandwich culture was performed as described previously (8) with slight modifications. Briefly, HUVECs ($1.1x10^5$ cells/cm^2) were sandwiched between two layers of collagen gel (0.258% type I collagen) with tube-induction medium composed of MCDB-104GK medium and 199 medium at a 13:7 ratio, supplemented with 2% FBS, l-ascorbic acid (25 μg/ml), penicillin (5 μg/ml), streptomycin (5 μg/ml) and neomycin (10 μg/ml) in 24-well culture plates (Becton Dickinson Labware) for 24 h. Tube formation was induced in the presence of tube-induction medium containing or stratifying culture supernatants derived from NSCLC cell lines, recombinant human VEGF-A (rhVEGF-A; HumanZyme), rhHDGF (Abnova) or rhFGF-2 (Fuji Film Wako Pure Chemical Corp.). Inhibitory analysis of tube formation was performed using tube-induction medium containing or stratifying the supernatants or the rhGFs together with neutralising antibodies listed in Table SI. Tube formation was quantified as described previously (8). Tube areas were quantified as the ratio of the area of the formed tubes to that of the imaged field using the Scion Image 4.0.3 program (Scion Corp.), and the ratio of tube areas of vehicle treatment or control was regarded as 1.0.

Cell viability analysis of three-dimensional (3D) culture of HUVECs. Tube formation of HUVECs in 3D culture was performed as described previously (8) with slight modifications. Briefly, HUVECs were trypsinised and spun down. The culture supernatants were aspirated, and the cell pellets were mixed with 0.258% type I collagen gels as described above. HUVECs mixed with collagen gel were added to each well ($2.86x10^6$ cells/ml) of 96-well culture plates (Becton Dickinson Labware) for cell viability analysis as described below. The plates were incubated at 37˚C for 1 h to allow the collagen gel to solidify. HUVECs were then incubated for 24 h to induce tube formation in the abovementioned tube-induction medium containing EBC-1 supernatants at 2-50 μg/ml. Cell viabilities were determined using the Cell Counting Kit-8 (Dojindo) as described previously (8). Cell viability assays in 3D culture were performed in triplicate.

Cell proliferation analysis of HUVECs in monolayer culture. Cell proliferation was analysed as described previously (8) with slight modifications. Briefly, HUVECs ($5.0x10^3$ cells/cm^2) in collagen-coated 24-well culture plates were treated with the abovementioned tube-induction medium containing EBC-1 supernatants (2-50 μg/ml) at the indicated time points. The cells were harvested by trypsinisation, and the cell counts were determined with the Coulter Counter Z1 (Coulter Japan). Cell proliferation assays were performed in duplicate.

Western blotting and antibodies. Western blotting was performed as described previously (8) with slight modifications. Briefly, HUVECs ($1x10^5$ cells/cm^2) were seeded in collagen-coated 60-mm culture dishes and incubated in the culture medium. The culture medium was aspirated after 24 h and the dishes were washed with PBS. HUVECs were then incubated in tube-induction medium without FBS for 3 h before stimulation. Stimulation was achieved by supplementing the serum-free tube-induction medium containing EBC-1 supernatant (50 μg/ml), 3D culture supernatant derived from Lu99 cells described below or rhVEGF-A (30 ng/ml) with or without a mouse monoclonal anti-IgG2B antibody (10 μg/ml) or an anti-VEGF-A neutralising antibody (10 μg/ml) at the indicated time points. After the stimulations, proteins were extracted from HUVECs. Culture supernatants were collected from serum-free cultures of EBC-1 cells and 3D culture of Lu99 cells treated with small interfering RNA (siRNA) described below. Protein concentration of each supernatant was determined using the Bradford method. Proteins extracted from HUVECs, siRNA-treated EBC-1 supernatants (50 μg) and siRNA-treated Lu99 cells were used for western blotting as described previously (8). The antibodies used for western blotting are described in Table SI.

RNA interference (RNAi) in NSCLC cell lines. Stealth RNAi Negative Control Duplexes (#12935-113) were purchased from Thermo Fisher Scientific, Inc. and used as a control. Each Stealth siRNA duplex oligoribonucleotide against VEGF-A, midkine (MK), HDGF, granulin (GRN) and FGF-2 (GenBank™ accession nos. NM_003376, NM_00101233, NM_004494, NM_002087 and NM_002006, respectively) were synthesised by Thermo Fisher Scientific, Inc. (sequences shown in Table SII). The duplex oligoribonucleotides were dissolved in diethyl pyrocarbonate-treated water to 20 μM. EBC-1 and Lu99 cells were transfected with siRNAs using Lipofectamine RNAiMAX (Thermo Fisher Scientific, Inc.) in accordance with the manufacturer's instructions. Stealth RNAi compounds were transfected at a final concentration of 5 nM in culture medium as described previously (8) with slight modifications. Briefly, $1x10^6$ cells were incubated overnight in 100-mm dishes containing 10 ml of RPMI-1640 medium supplemented with 10% FBS without penicillin, streptomycin and neomycin. Lipofectamine RNAiMAX and siRNA were each diluted in 1 ml of RPMI-1640 medium for 5 min at room temperature, and then they were combined and incubated for 15 min at room temperature to form complexes. Two millilitre of the mixture was added to each dish and the cells were further incubated. The old RPMI-1640 medium containing the mixture was aspirated after a 48-h incubation, the dishes were washed with PBS, and 10 ml of fresh RPMI-1640 medium supplemented with 10% FBS was added and incubated for another 24 h (a total of 72-h incubations after starting the siRNA transfections). The cells were harvested by trypsinisation. EBC-1 cells were then seeded at a density of $2x10^5$ cells/cm^2 in 35-mm, 60-mm or 100-mm dishes in serum-free MCDB-104GK medium supplemented with penicillin, streptomycin and neomycin and incubated further for 24 h as described above. The serum-free culture supernatants from siRNA-treated EBC-1 cells were collected after the 24-h incubations (a total of 96-h incubations after starting the siRNA transfection). Following trypsinisation, Lu99 cells were incubated in 3D cultures as described below.

Enzyme-linked immunosorbent assay (ELISA) for VEGF-A. The levels of VEGF-A protein in serum-free culture supernatants (50 μg/ml) from EBC-1 cells treated with or without siRNAs were measured using the Human VEGF-A ELISA Kit (RayBiotech, Inc.) according to the manufacturer's instructions as described previously (8).

Identification of proteins by mass spectrometry (MS). After EBC-1 supernatant was collected as described above, 20 μl ($\geq$1 mg/ml) of each supernatant was precipitated using trichloroacetic acid. The precipitates derived from each supernatant were dissolved in Tris buffer (2 mM EDTA/250 mM Tris-HCl) at pH 8.5, reduced with 0.67 M dithiothreitol, alkylated with 1.4 M iodoacetamide and digested with trypsin. The recovered peptides were analysed using a Q Exactive Plus MS instrument (Thermo Fisher Scientific, Inc.) coupled with a capillary high-performance liquid chromatography system (EASY-nLC 1200, Thermo Fisher Scientific, Inc.) to acquire MS/MS spectra. A 0.075x150 mm-EASY-Spray column (3-μm particle diameter, 100-Å pore size, Thermo Fisher Scientific, Inc.) was used with mobile phases of 0.1% formic acid and 0.1% formic acid/80% acetonitrile. Data derived from the MS/MS spectra were searched in the SWISS-Prot database using the MASCOT Server (http://www. matrixscience. com) and proteins were identified using the Scaffold viewer program (http://www.proteomesoftware. com/products/scaffold). Protein identification by MS was performed in two independent experiments, and proteins identified in both experiments are shown in Table SIII.

ELISA for HDGF. The levels of HDGF protein in EBC-1 supernatants (50 μg/ml) and those in Lu99 supernatants were measured using the Human HDGF ELISA Kit (Arigo biolaboratories Corp., Hsinchu, Taiwan) according to the manufacturer's instructions. Briefly, each microtitre plate was pre-coated with a polyclonal anti-human HDGF antibody (Arigo Biolaboratories Corp.). After collecting the supernatants, EBC-1 supernatants (50 μg/ml), Lu99 supernatants or rhHDGF (Arigo biolaboratories Corp.) were added to each well for 2 h at 37°C. After 3 washes with wash buffer, 100 μl of peroxidase-linked anti-HDGF antibody (ARG81356, Arigo biolaboratories Corp.) was added to each well for 1 h at 37°C. Detection was performed with tetramethyl-benzidine, dihydrochloride, dihydrate and hydrogen peroxide. The measurements were repeated in duplicate. The lowest concentration of HDGF detected by this system was 30 pg/ml. The colour intensity of each solution after development was quantified using a

SpectraMax PLUS 384 microplate reader (Molecular Devices, Sunnyvale, CA).

Semi-quantitative real-time reverse transcription-polymerase chain reaction (RT-qPCR). Isolation of total RNA, synthesis of first-strand cDNA and PCR were performed as described previously (8) with slight modifications. Briefly, total RNAs from EBC-1, A549 and Lu99 cells were isolated using the TRIzol reagent (Enzo Life Sciences Inc.). First-strand cDNA was synthesised from total RNA (1.25 μg) using the PrimeScript RT Reagent Kit (Takara Bio, Inc.). PCR was performed with the synthesised cDNA products using TaqMan Gene Expression Master Mix (Thermo Fisher Scientific, Inc.) for each target gene. All reactions were carried out in triplicate. The sequences of the PCR primer pairs and fluorogenic probes used for HDGF, glyceraldehyde-3-phosphate dehydrogenase (GAPDH), 18S-rRNA, VEGF-A, brain-derived neurotrophic factor (BDNF), FGF-2 and FGF-5 are available on the Thermo Fisher Scientific website (http://www.thermofisher.com, HDGF assay ID: Hs00610314_m1; GAPDH assay ID: Hs99999905_m1; 18S-rRNA assay ID: Hs99999901_s1; VEGF-A assay ID: Hs00900054_m1; BDNF assay ID: Hs00380947_m1; FGF-2 assay ID: Hs00266645_m1; FGF-5 assay ID: Hs00170454_m1). The PCR products were analysed using the ABI 7500 real-time PCR system (Thermo Fisher Scientific. Inc.) and quantified by employing the $2^{-\Delta\Delta Cq}$ quantification method (9). As internal controls, the expression levels of HDGF mRNA in EBC-1 cells cultured with or without FBS were normalised to corresponding expression levels of GAPDH mRNA, and those of HDGF, VEGF-A, BDNF, FGF-2 and FGF-5 mRNAs in the NSCLC cell lines were normalised to the corresponding expression levels of 18S-rRNA.

Gene microarray analysis. Isolation of total RNA from EBC-1 and Lu99 cells was performed as described above. The degrees of RNA cross-linking and RNA degradation were analysed by electrophoresis using the Agilent 2100 Bioanalyzer (Agilent Technologies). Microarray analysis was performed with the 3D-Gene Human Oligo Chip 25k (Toray Industries Inc.). For efficient hybridisation, this microarray was designed with a columnar structure to stabilise spot morphologies and to enable micro-bead agitation. Total RNA (0.5 μg) isolated from EBC-1 and Lu99 cells was amplified using the Amino Allyl MessageAMP II aRNA Amplification Kit (Applied Biosystems). Amplified RNAs derived from EBC-1 and Lu99 cells (10 μg) were labeled with Cyanine 5 (Cy5) and Cy3, respectively. Purified Cy5- and Cy3-labeled aRNA pools (each 1 μg) were individually mixed with hybridisation buffer, and hybridised at 37°C for 16 h. The hybridisation was performed according to the manufacturer's instructions (www.3d-gene.com). The hybridisation signals were obtained using the 3D-Gene Scanner (Toray Industries Inc.) and processed using the 3D-Gene Extraction software (Toray Industries Inc.). The signals detected for each gene were normalised using global normalisation method.

Three-dimensional culture of Lu99 cells. Lu99 cells were trypsinised and spun down, the culture supernatants were aspirated, and the cell pellets were mixed with 0.258% type I collagen gels as described above. Collagen gel (42 or 350 μl)

was added to each well of 96- or 24-well culture plates, respectively, and the plates were incubated at 37°C for 3 h to allow the collagen gel to solidify. The abovementioned tube-induction medium was added to each well for a total of 120 μl (96-well plates) or 1 ml (24-well plates) at cell densities of 0-5x10^6 cells/ml for cell viability analysis or collecting 3D culture supernatants derived from Lu99 cells. Lu99 cells in 3D culture were incubated in 24-well culture plates for 24 h, each supernatant was then collected, and 500 μl of each supernatant was stratified in tube-induction medium to induce tube formation in sandwich culture described above. Cell viability was determined using the Cell Counting Kit-8 (Dojindo, Japan) as described previously (8). Cell viability assays in 3D culture were performed in triplicate. Protein concentrations in 3D culture supernatant derived from Lu99 cells cultured at a cell density of 2x10^6 cells/ml (Lu99 supernatant) were determined using the Bradford method.

Quantification and statistical analysis. All data are presented as means ± standard errors of the means (SEMs, n=3) of three independent experiments. Differences in mean values among groups for multiple comparisons were subjected to one-way factorial ANOVA and subsequent Dunnett's test or Tukey's test, and were considered significant when P-values were <0.05 (*P<0.05, **P<0.01, ***P<0.005 and ****P<0.001) as indicated in the figures and legends by the relevant symbol. Statistical analyses were performed using JMP Pro 13 (SAS Institute Inc., Japan).

Results

Serum-free culture supernatant derived from a human NSCLC cell line, EBC-1, induces tube formation. To identify angiogenic factors in NSCLC, we performed serum-free culture in this study, based on our previous study where angiogenic factors were identified on human mesothelioma cells (8). As shown in Fig. 1A, spheroid-like aggregation and cell shrinkage-like cell death were observed at 24 h after serum-free culture in human NSCLC cell lines, A549 and Lu99. Meanwhile, the serum-free culture induced neither the aggregation nor cell death in another NSCLC cell line, EBC-1 (Fig. 1A and B). These results indicate that EBC-1 cells can adapt to serum-free culture.

We examined the effects of serum-free culture supernatant derived from EBC-1 cells (EBC-1 supernatant) on angiogenesis. EBC-1 supernatant induced the tube formation of HUVECs (Fig. 1C) and increased the cell viability of HUVECs in 3D cultures (Fig. S1A) for 24 h in concentration-dependent manners. The numbers of HUVECs in monolayer cultures were significantly increased by EBC-1 supernatant after 48-h or 72-h incubations, but not after a 24-h incubation (Fig. S1B). These results indicate that EBC-1 supernatant induces tube formation and suggest that the increase in cell viability of HUVECs by EBC-1 supernatant is due to suppressed cell death rather than to promotion of cell proliferation.

EBC-1 supernatant-induced tube formation is mediated by both VEGF-dependent and -independent pathways. We then examined VEGFR2 phosphorylation in HUVECs treated
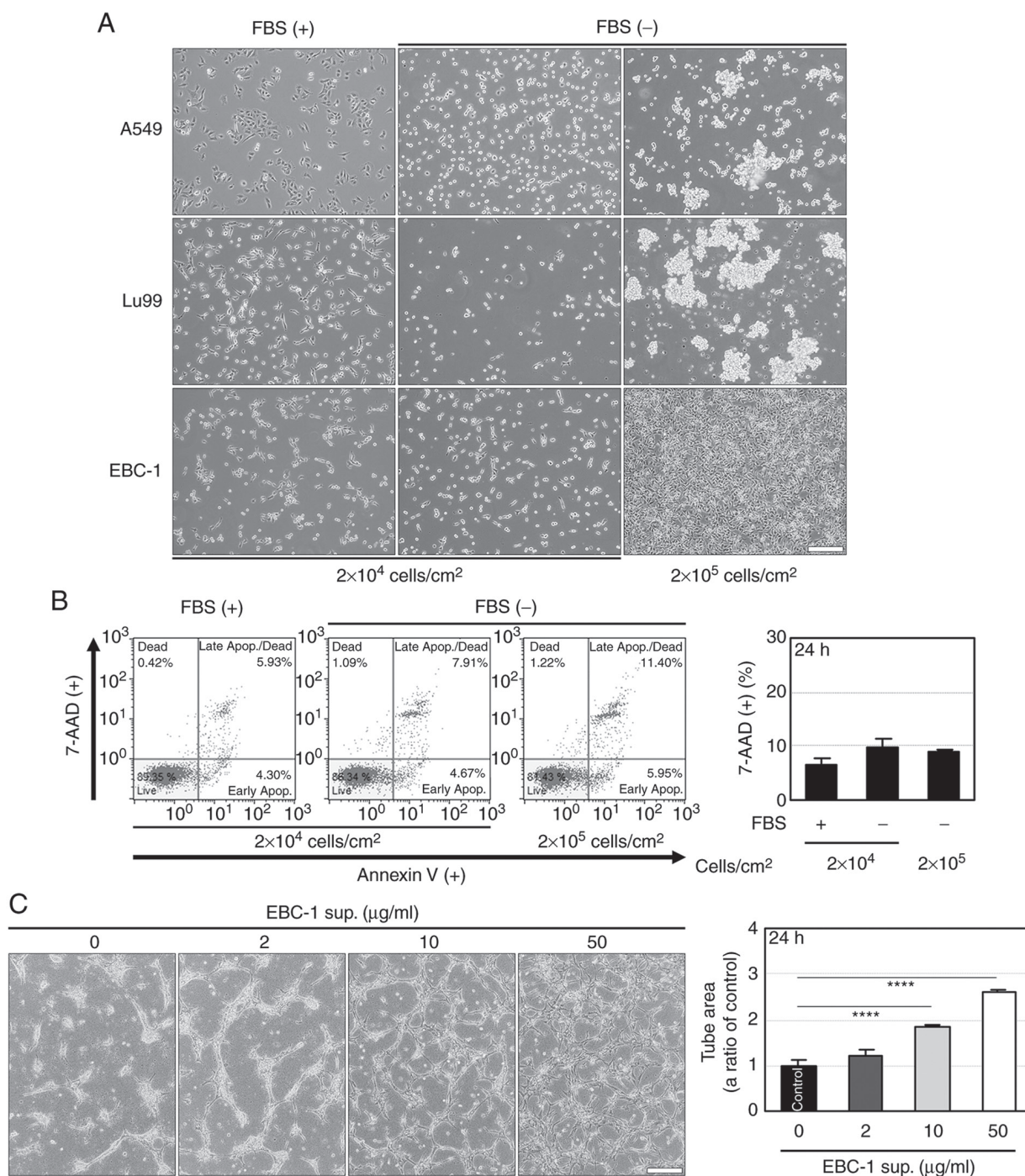
Figure 1. EBC-1 supernatant (sup.) induces angiogenesis. (A) Spheroid-like aggregation and cell shrinkage is induced by serum-free culture in A549 and Lu99 cells, but not in EBC-1 cells. Human NSCLC cell lines, A549, Lu99 and EBC-1, were incubated with or without FBS for 24 h as described in Materials and methods. (B) Flow cytometric analysis using double staining with Annexin V and 7-AAD. EBC-1 cells were incubated in monolayer cultures with or without FBS for 24 h, and then flow cytometric analysis was performed using double staining with Annexin V and 7-AAD as described in Materials and methods. (C) EBC-1 supernatant induces tube formation of HUVECs in 3D culture. HUVECs sandwiched between two layers of collagen were incubated with EBC-1 supernatant at the indicated concentrations for 24 h as described in Materials and methods. ****P<0.001. Each assay was performed in three independent experiments and representative images are shown. Data represent the means ± SEMs of three independent experiments. Statistically significant differences were determined by using one-way factorial analysis of variance (ANOVA)-Dunnett's test. Scale bar, 100 μm. NSCLC, non-small cell lung cancer; HUVECs, human umbilical vein endothelial cells.

with EBC-1 supernatant. EBC-1 supernatant transiently phosphorylated VEGFR2 and ERK1/2 (Fig. 2A). An anti-VEGF-A antibody (10 μg/ml) significantly, but not completely, suppressed EBC-1 supernatant-induced tube formation (Fig. 2B). In addition, the antibody markedly suppressed the phosphorylation of VEGFR2, but not completely that of ERK1/2 (Fig. 2C).

We also performed RNAi using a siRNA targeting VEGF-A (siVEGF-A) in EBC-1 cells. Treatment of EBC-1 cells with siVEGF-A did not induce cell death more significantly than those with vehicle or control siRNA (siControl, Fig. S2). ELISA for VEGF-A showed that the mean VEGF-A concentration in the supernatant (50 μg/ml) was 16.47±2.65 ng/ml (Fig. 3A). We
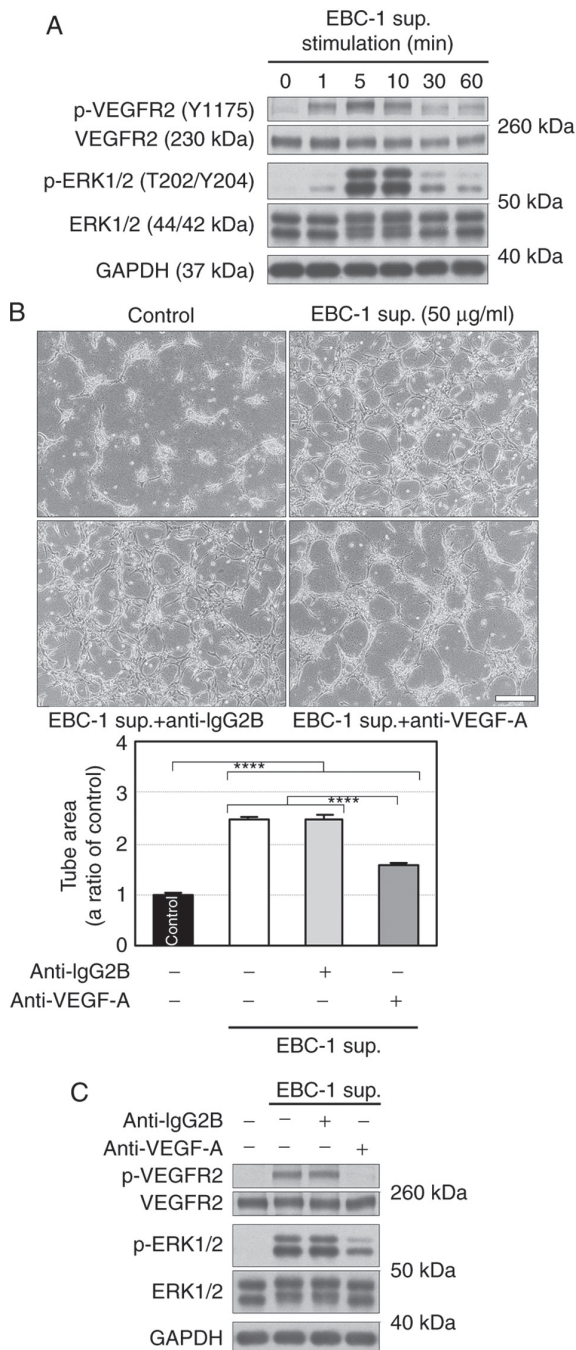
Figure 2. EBC-1 supernatant (sup.) induces tube formation mediated by both VEGF-A and VEGF-independent angiogenic factors. (A) EBC-1 supernatant transiently induces phosphorylation of VEGFR2 and ERK1/2. HUVECs in collagen-coated culture dishes were incubated with EBC-1 supernatant at 50 μg/ml at the indicated time points in monolayer cultures, and cell extract was then prepared from the cells as described in Materials and methods. (B) VEGF-A neutralisation partially suppresses EBC-1 supernatant-induced tube formation. HUVECs sandwiched between two layers of collagen were incubated with EBC-1 supernatant (50 μg/ml) alone and that together with the mouse monoclonal anti-IgG2B (10 μg/ml) or the anti-VEGF-A antibody for 24 h. ****P<0.001. (C) EBC-1 supernatant-induced phosphorylation of ERK1/2 is partially suppressed by VEGF-A neutralisation. HUVECs in collagen-coated culture dishes were incubated with EBC-1 supernatant (50 μg/ml) alone and that together with the mouse monoclonal anti-IgG2B (10 μg/ml) or the anti-VEGF-A antibody for 5 min. Cell extract was then prepared from the cells. Each assay was performed in three independent experiments and representative images are shown. Data represent the means ± SEMs of three independent experiments. Statistically significant differences were determined by using one-way factorial ANOVA-Tukey's test. Scale bar, 100 μm. VEGF, vascular endothelial growth factor; VEGFR2, vascular endothelial growth factor receptor 2; HUVECs, human umbilical vein endothelial cells.

previously reported that the anti-VEGF-A antibody (10 μg/ml) completely abrogated tube formation and VEGFR2 phosphorylation induced by VEGF-A (30 ng/ml) (8). The result of ELISA for VEGF-A and our previous findings indicate that the anti-VEGF-A antibody completely inhibited VEGF-dependent tube formation. ELISA also showed that siVEGF-A significantly abrogated VEGF-A secretion (Fig. 3A). Furthermore, the serum-free culture supernatant derived from EBC-1 cells transfected with siVEGF-A significantly, but not completely, suppressed tube formation (Fig. 3B). These results suggest that EBC-1 supernatant-induced tube formation is regulated by both VEGF-dependent and -independent pathways.

VEGF and HDGF regulate EBC-1 supernatant-induced tube formation. To explore humoral factors that regulate EBC-1 supernatant-induced tube formation independently of VEGF-A, we analysed proteins in the supernatant by using mass spectrometry (MS) and identified 1,007 proteins (Table SIII), most related to adhesion, cytoskeletal and nuclear proteins, indicating that there were microvesicles such as exosomes in the EBC-1 supernatant (10,11). Among the proteins, interleukin-8 (IL-8) (12), macrophage migration inhibitory factor (MIF) (13), galectin-1 (14), MK (15), IL-18 (16), galectin-3 (17), HDGF (18), osteopontin (OPN) (19), connective tissue growth factor (CTGF) (20) and GRN (21) are known to be involved in angiogenesis besides VEGF-A. We examined the involvements of IL-8, MIF, galectin-1, IL-18, galectin-3, OPN and CTGF in EBC-1 supernatant-induced tube formation using commercially available neutralising antibodies corresponding to each of the above proteins or their receptors. None of the antibodies suppressed EBC-1 supernatant-induced tube formation (Fig. S3), suggesting that IL-8, MIF, galectin-1, IL-18, galectin-3, OPN and CTGF are not directly involved in EBC-1 supernatant-induced tube formation.

We then performed RNAi using siRNAs targeting MK (siMK), HDGF (siHDGF) and GRN (siGRN) in EBC-1 cells and investigated the involvements of these three proteins in EBC-1 supernatant-induced tube formation. Each siRNA and siControl did not induce cell death in EBC-1 cells compared to vehicle in the 24-h serum-free cultures (Fig. S4A). We also confirmed that each siRNA abrogated secretion of the protein corresponding to the target gene (Fig. 4A). The supernatant of EBC-1 cells transfected with HDGF siRNA (siHDGF) significantly, but not completely, suppressed tube formation compared to those treated with vehicle or other siRNAs (Fig. 4B).

We further investigated the involvement of HDGF in EBC-1 supernatant-induced tube formation using another siHDGF (#761). siHDGF#761 did not induce cell death in EBC-1 cells compared to vehicle and siControl (Fig. S4B) and abrogated HDGF secretion in 24-h serum-free cultures (Fig. 5A). Similar to the result shown in Fig. 4B, the supernatant of EBC-1 cells transfected with siHDGF#761 significantly, but not completely, suppressed tube formation compared to those treated with vehicle or siControl (Fig. 5B). We also investigated the effect of HDGF on tube formation using rhHDGF. rhHDGF (10 ng/ml) significantly induced tube formation, but much less potently than did the EBC-1 supernatant (Fig. 5C).

ELISA for HDGF showed that the mean HDGF concentration in EBC-1 supernatant (50 μg/ml) was 1.67±0.26 ng/ml
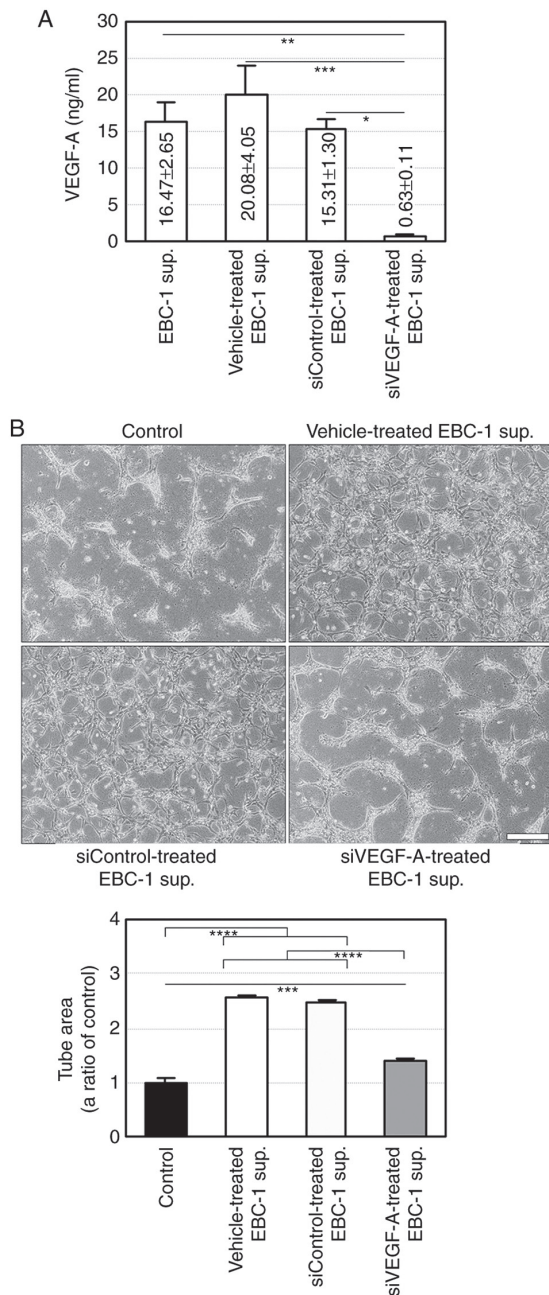
Figure 3. VEGF-A knockdown partially inhibits tube formation induced by EBC-1 supernatant. (A) ELISA for VEGF-A in EBC-1 supernatant. The levels of VEGF-A protein in serum-free culture supernatants (50 µg/ml) of EBC-1 cells and those of the cells transfected with vehicle, siControl or siVEGF-A (#1150) were measured using the Human VEGF-A ELISA Kit as described in Materials and methods. [*]P<0.05, [**]P<0.01 and [***]P<0.005. (B) VEGF-A in EBC-1 supernatant partially induces tube formation. HUVECs sandwiched between two layers of collagen were incubated with serum-free culture supernatants (50 µg/ml) of EBC-1 cells transfected with vehicle, siControl or siVEGF-A (#1150) for 24 h. [***]P<0.005 and [****]P<0.001. Each assay was performed in three independent experiments and representative images are shown. Data represent the means ± SEMs of three independent experiments. Statistically significant differences were determined by using one-way factorial ANOVA-Tukey's test. Scale bar, 100 µm. VEGF, vascular endothelial growth factor; HUVECs, human umbilical vein endothelial cells.

(Table SIV), while HDGF mRNA was expressed in the EBC-1 cells independently of the presence of FBS (Fig. 6A). In addition, the expression levels of HDGF mRNA in A549 and Lu99 cells were significantly higher than that in the EBC-1 cells
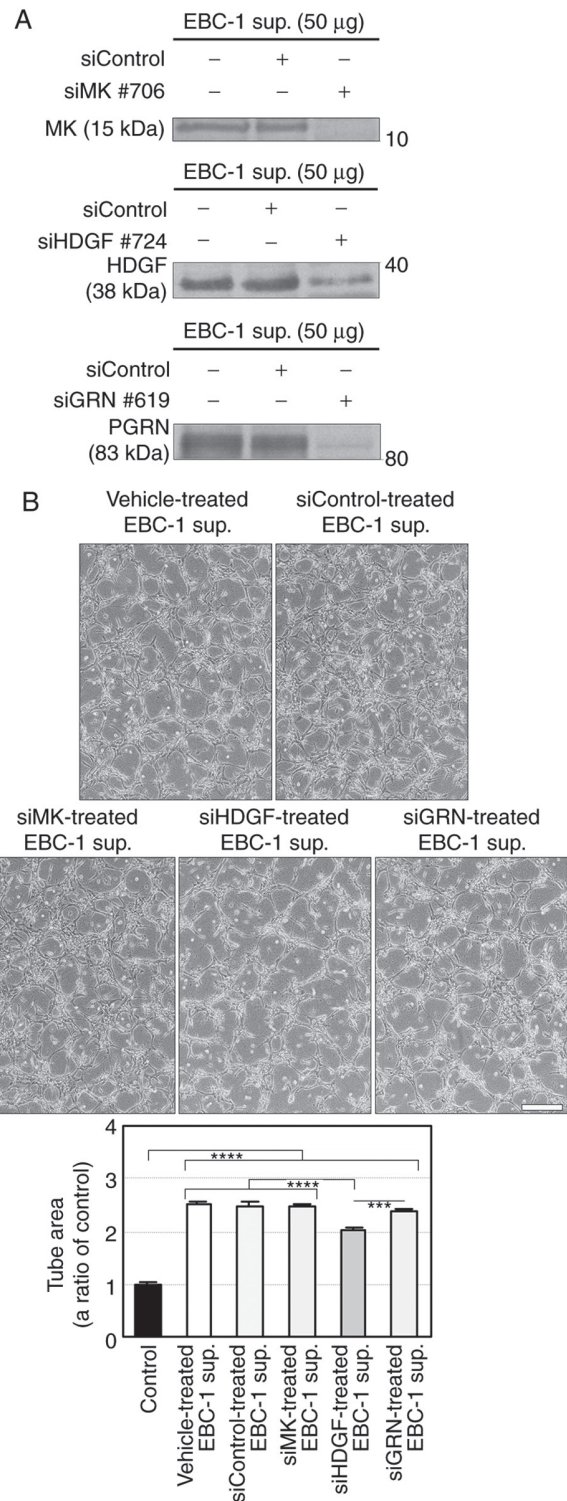
Figure 4. HDGF, but not MK and GRN, is involved in EBC-1 supernatant-induced tube formation. (A) Knockdown of MK, HDGF and GRN by RNAi in the EBC-1 supernatant (sup.). Serum-free culture supernatants (50 µg) of EBC-1 cells transfected with vehicle, siControl, siMK (#706), siHDGF (#724) or siGRN (#619) were used for western blotting. (B) HDGF, but not MK and GRN, is involved in EBC-1 supernatant-induced tube formation. HUVECs sandwiched between two layers of collagen were incubated with serum-free culture supernatants (50 µg/ml) of EBC-1 cells transfected with vehicle, siControl, siMK (#706), siHDGF (#724) or siGRN (#619) for 24 h. [***]P<0.005 and [****]P<0.001. Each assay was performed in three independent experiments and representative images are shown. Data represent the means ± SEMs of three independent experiments. Statistically significant differences were determined by using one-way factorial ANOVA-Tukey's test. Scale bar, 100 µm. HDGF, hepatoma-derived growth factor; MK, midkine; GRN, granulin; HUVECs, human umbilical vein endothelial cells.
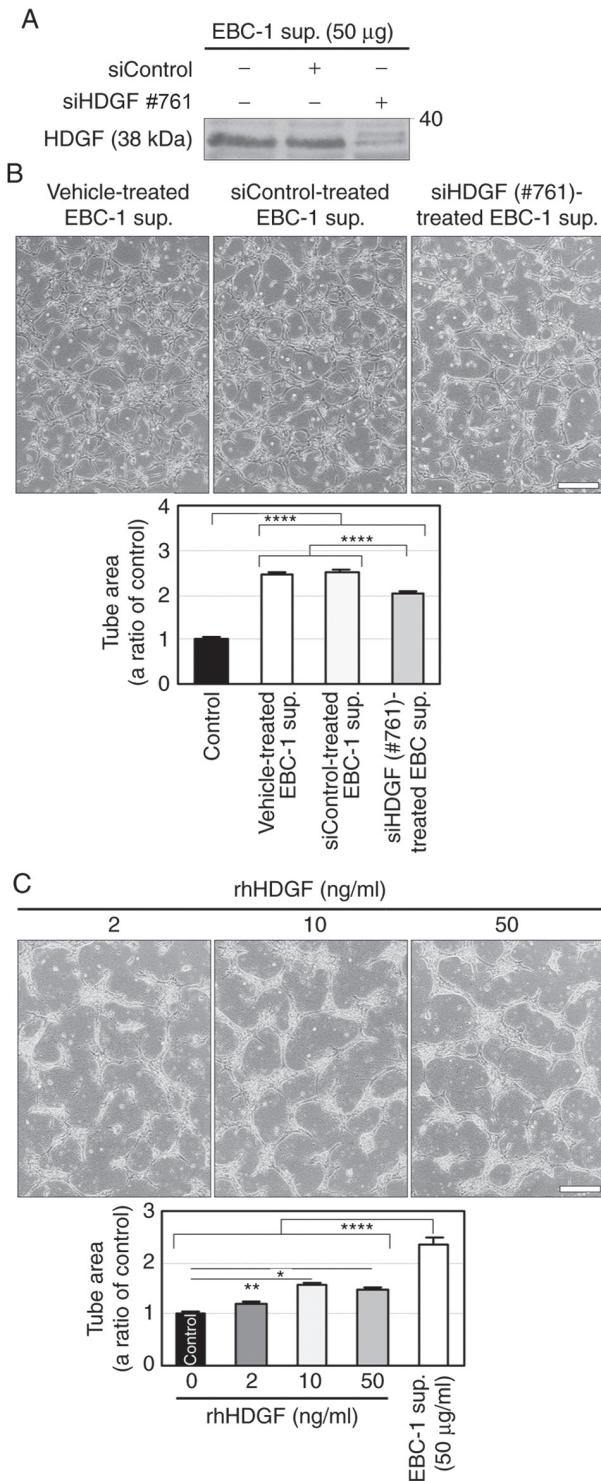
A

B

C

Figure 5. HDGF is directly involved in EBC-1 supernatant-induced tube formation. (A) HDGF knockdown by another HDGF siRNA in the EBC-1 supernatant (sup.). Serum-free culture supernatants (50 µg) of EBC-1 cells transfected with vehicle, siControl or siHDGF (#761) were used for western blotting. (B) HDGF in EBC-1 supernatant partially induces tube formation. HUVECs sandwiched between two layers of collagen were incubated with serum-free culture supernatants (50 µg/ml) of EBC-1 cells transfected with vehicle, siControl or siHDGF (#761) for 24 h. ****P<0.001. (C) rhHDGF partially induces tube formation. HUVECs sandwiched between two layers of collagen were incubated with rhHDGF at 2, 10 and 50 ng/ml or with EBC-1 supernatant (50 µg/ml) for 24 h. *P<0.05, **P<0.01 and ****P<0.001. Each assay was performed in three independent experiments and representative images are shown. Data represent the means ± SEMs of three independent experiments. Statistically significant differences were determined by using One-way factorial ANOVA-Tukey's test. HDGF, hepatoma-derived growth factor; HUVECs, human umbilical vein endothelial cells.

(Fig. 6B). Furthermore, additions of the anti-VEGF-A antibody to the supernatants of EBC-1 cells transfected with siHDGFs (#724 or #761) suppressed tube formation more significantly than those of the antibody to the supernatants of the cells treated with vehicle or siControl (Fig. 6C). These results indicate that VEGF mainly regulates EBC-1 supernatant-induced tube formation and HDGF enhances VEGF-dependent tube formation.

Three-dimensional culture supernatant derived from Lu99 cells induces HDGF- and VEGF-independent tube formation. To determine whether HDGF is involved in angiogenesis induced by the other NSCLC cell lines, we established a novel culture method; NSCLC cells were embedded in collagen gel and cultured three-dimensionally in tube-induction medium containing FBS (Fig. 7A). The 3D culture supernatants derived from Lu99 cells incubated at 0-5x10^6 cells/ml for 24 h significantly induced tube formation in a cell density-dependent manner, whereas no significant differences were noted in tube formation when using different cell densities (2-5x10^6 cells/ml; Fig. 7B). Thus, we used the supernatant derived from Lu99 cells cultured at a cell density of 2x10^6 cells/ml (Lu99 supernatant) in subsequent experiments.

We performed RNAi in Lu99 cells using siHDGFs (#724 or #761) and investigated the involvement of HDGF in Lu99 supernatant-induced tube formation. Both siHDGFs (#724 or #761) had little effects on cell viability of Lu99 cells in 3D cultures (Fig. 7C) and on protein concentrations in Lu99 supernatants (Fig. 7D), and markedly abrogated HDGF secretion (Fig. 7E) compared to treatments with vehicle and siControl. However, the supernatants derived from Lu99 cells transfected with siHDGFs did not suppress tube formation (Fig. 7F), although the HDGF concentrations in EBC-1 and Lu99 supernatants were almost the same (Table SIV and Fig. 7E). The reason why HDGF was not directly involved in Lu99 supernatant-induced tube formation was presumed to be due to a decrease in HDGF concentration by stratification of the Lu99 supernatant in the tube-induction medium (Fig. 7E). These results suggest an involvement of more potent angiogenic factors than HDGF in Lu99 supernatant-induced tube formation.

We also investigated the expression levels of VEGF-A mRNA in EBC-1, A549 and Lu99 cells. Intriguingly, VEGF-A mRNA expression in Lu99 cells was significantly weaker than those in EBC-1 and A549 cells (Fig. 8A). The Lu99 supernatant did not induce VEGFR2 phosphorylation (Fig. 8B). In addition, the anti-VEGF-A antibody failed to suppress Lu99 supernatant-induced tube formation (Fig. 8C). These results indicate that the Lu99 supernatant induces HDGF- and VEGF-independent tube formation.

FGF-2 regulates Lu99 supernatant-induced tube formation. To explore the humoral factor that regulates Lu99 supernatant-induced tube formation, we comprehensively analysed mRNA expression in Lu99 and EBC-1 cells by using gene microarray, and thereby identified 61 mRNAs expressed in Lu99 cells, but not in EBC-1 cells (Table SV). Among these mRNA-encoded proteins, brain-derived neurotrophic factor (BDNF) (22), FGF-2 (23) and FGF-5 (24) are secreted extracellularly and are known to be involved in angiogenesis. The
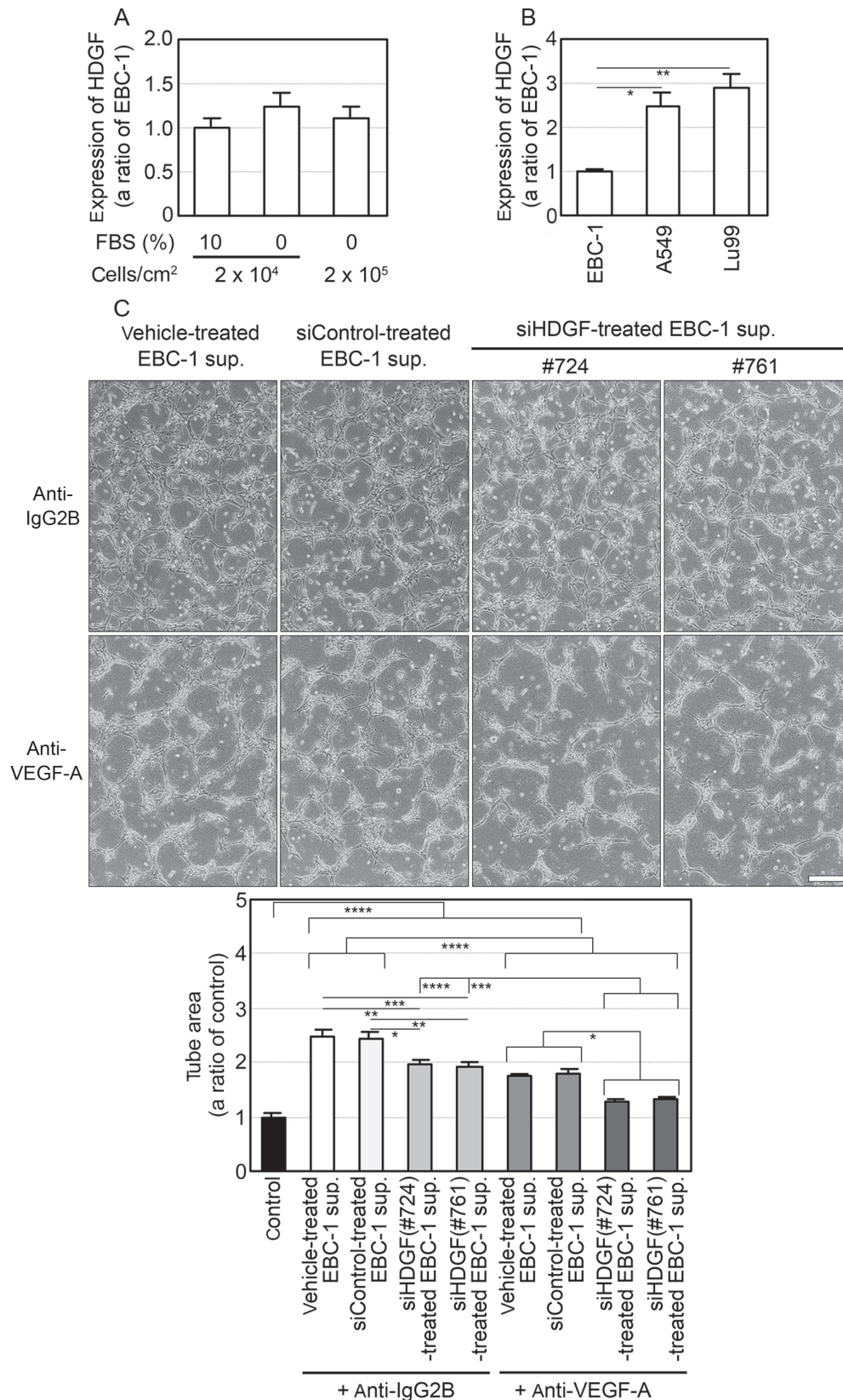
Figure 6. VEGF-A and HDGF regulate tube formation induced by the EBC-1 supernatant (sup.). (A and B) Expression of HDGF mRNA in human NSCLC cells. Each total RNA was isolated from EBC-1 cells at the indicated cell densities with or without 10% FBS (A) and from EBC-1, A549 and Lu99 cells incubated with 10% FBS (B) for 24 h. Synthesis of first-strand cDNA and PCR were then performed as described in Materials and methods. The expression levels of HDGF mRNA were normalised to the corresponding levels of GAPDH mRNA (A) and those of 18S-rRNA (B) as an internal control. $^{*}P<0.05$ and $^{**}P<0.01$ (B). (C) VEGF-A and HDGF in EBC-1 supernatant induce tube formation. HUVECs sandwiched between two layers of collagen were incubated with serum-free culture supernatants (50 μg/ml) of EBC-1 cells transfected with vehicle, siControl, siHDGF (#724) or siHDGF (#761) together with the mouse monoclonal anti-IgG2B (10 μg/ml) or the anti-VEGF-A antibody. $^{*}P<0.05$, $^{**}P<0.01$, $^{***}P<0.005$ and $^{****}P<0.001$. Each assay was performed in three independent experiments and representative images are shown. Data represent the means ± SEMs of three independent experiments. Statistically significant differences were determined by using one-way factorial ANOVA with Dunnett's test (A and B) and Tukey's test (C) Scale bar, 100 μm. VEGF, vascular endothelial growth factor; NSCLC, non-small cell lung cancer; HDGF, hepatoma-derived growth factor; HUVECs, human umbilical vein endothelial cells.
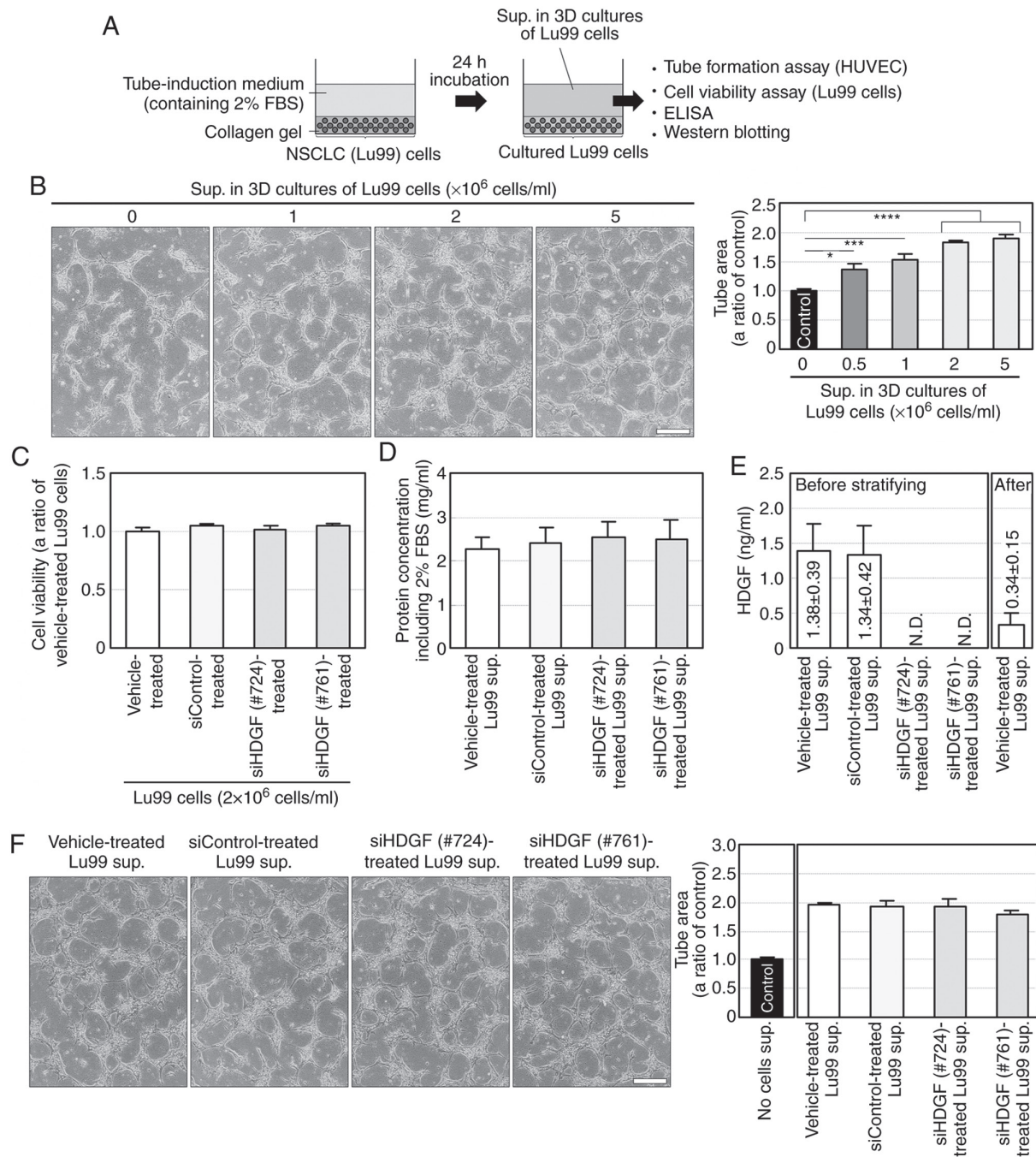
Figure 7. Lu99 supernatant (sup.) induces HDGF-independent tube formation. (A) Procedure of preparation and use of the supernatant derived from Lu99 cells in 3D culture. Lu99 cells embedded in collagen were three-dimensionally incubated with tube-induction medium containing 2% FBS for 24 h, and then Lu99 supernatant was collected as described in Materials and methods. (B) Lu99 supernatant induces tube formation in a cell-density-dependent manner. HUVECs sandwiched between two layers of collagen were incubated with tube-induction medium, in which 3D culture supernatants derived from Lu99 cells cultured at 0-5x10^6 cells/ml were stratified, for 24 h as described in Materials and methods. *P<0.05, ***P<0.005 and ****P<0.001. (C) Lu99 cell viability in 3D culture was not decreased by HDGF knockdown. Lu99 cells transfected with vehicle, siControl, siHDGF (#724) or siHDGF (#761) were three-dimensionally embedded in collagen and incubated in tube-induction medium for 24 h (a total of 96-h incubations after starting the siRNA transfections) as described in Materials and methods. (D) Protein concentration in Lu99 supernatants. After 24-h incubations in 3D cultures of Lu99 cells transfected with vehicle, siControl, siHDGF (#724) or siHDGF (#761), the culture supernatants derived from these cells were collected and protein concentrations in the supernatants were determined using the Bradford method as described in Materials and methods. (E) ELISA for HDGF in Lu99 supernatant. The levels of HDGF protein in 3D culture supernatants of Lu99 cells transfected with vehicle, siControl, siHDGF (#724) or siHDGF (#761) and that after stratifying vehicle-treated Lu99 supernatant in tube-induction medium were measured using the Human HDGF ELISA Kit as described in Materials and methods. N.D., not detectable. (F) HDGF is not directly involved in Lu99 supernatant-induced tube formation. HUVECs sandwiched between two layers of collagen were incubated with tube-induction medium, in which 3D culture supernatants of Lu99 cells transfected with vehicle, siControl, siHDGF (#724) or siHDGF (#761) were stratified, for 24 h. Each assay was performed in three independent experiments and representative images are shown. Data represent the means ± SEMs of three independent experiments. Statistically significant differences were determined by using one-way factorial ANOVA-Tukey's test. Scale bar, 100 μm. HDGF, hepatoma-derived growth factor; HUVECs, human umbilical vein endothelial cells.

expression levels of BDNF, FGF-2 and FGF-5 mRNAs were significantly higher in Lu99 cells than in EBC-1 and A549 cells (Fig. 9A). We then examined the involvements of BDNF, FGF-2 and FGF-5 in Lu99 supernatant-induced tube formation
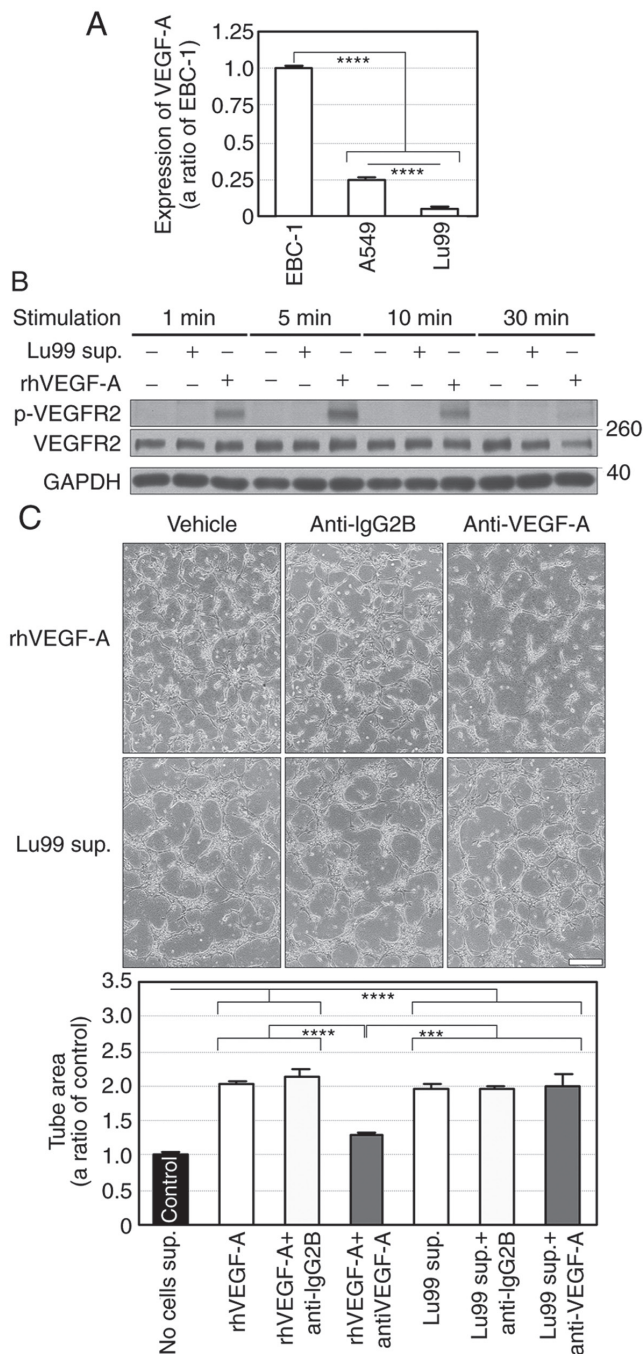
Figure 8. Lu99 supernatant (sup.) induces VEGF-independent tube formation. (A) Lu99 cells barely express VEGF-A mRNA. Total RNA was isolated from EBC-1, A549 and Lu99 cells incubated with 10% FBS for 24 h, and then synthesis of first-strand cDNA and PCR was performed. Each level of VEGF-A mRNA was normalised to the corresponding level of 18S-rRNA as an internal control. ****P<0.001. (B) VEGFR2 phosphorylation is not induced by Lu99 supernatant. HUVECs in collagen-coated culture dishes were incubated with tube-induction medium, in which Lu99 supernatant or rhVEGF-A (30 ng/ml) were stratified, at the indicated time points and cell extract was then prepared from the cells. (C) VEGF-A neutralisation failed to suppress Lu99 supernatant-induced tube formation. HUVECs sandwiched between two layers of collagen were incubated with tube-induction medium alone and that together with the mouse monoclonal anti-IgG2B antibody (10 µg/ml) or the anti-VEGF-A antibody, in which either rhVEGF-A (30 ng/ml) or Lu99 supernatant were stratified. ***P<0.005 and ****P<0.001. Each assay was performed in three independent experiments and representative images are shown. Data represent the means ± SEMs of three independent experiments. Statistically significant differences were determined by using one-way factorial ANOVA-Tukey's test. Scale bar, 100 µm. VEGF, vascular endothelial growth factor; HUVECs, human umbilical vein endothelial cells; VEGFR2, vascular endothelial growth factor receptor 2.

using commercially available neutralising antibodies corresponding to each of the above proteins. Consequently, Lu99 supernatant-induced tube formation was not suppressed by antibodies to BDNF and FGF-5, but was markedly inhibited by that to FGF-2 (Fig. 9B). As expected, rhFGF-2 (≥3 ng/ml) induced tube formation as potently as did Lu99 supernatant (Fig. S5). We further confirmed the involvement of FGF-2 in Lu99 supernatant-induced tube formation using another monoclonal anti-FGF-2 neutralising antibody. Similar to the result shown in Fig. 9B, the antibody significantly inhibited Lu99 supernatant-induced tube formation (Fig. 9C). These results indicate that FGF-2 regulates HDGF- and VEGF-independent tube formation induced by Lu99 supernatant.

Discussion

In the present study, we demonstrated for the first time that hepatoma-derived growth factor (HDGF) enhances angiogenesis in non-small cell lung cancer (NSCLC) cells expressing vascular endothelial growth factor (VEGF) and that fibroblast growth factor-2 (FGF-2) is a VEGF-independent angiogenic factor in VEGF-downregulated NSCLC cells (Fig. 10). Our established serum-free and 3D culture methods revealed the direct involvement of HDGF and FGF-2 in NSCLC-induced angiogenesis. These novel findings may prove to be useful in developing antiangiogenic therapy to neutralise HDGF or FGF-2 in NSCLC.

HDGF is a secretory heparin-binding growth factor purified from conditioned medium in which a human hepatoma cell line (HuH-7) was cultured (25) and involved in tumour-associated events such as tumourigenesis, metastasis and angiogenesis (18). HDGF is also known to be expressed endogenously in endothelial cells and to induce angiogenesis exogenously (26). It has been shown that numerous NSCLC cell lines and primary NSCLC specimens express HDGF (27,28) and that patients with NSCLC expressing high HDGF present with a poor prognosis compared with those expressing low HDGF (28,29). Recently, downregulation of microRNAs, which target multiple genes containing HDGF, was reported to promote tumour growth and invasion of primary cells or cell lines including A549 in NSCLC (30-32). Glioblastoma stem-like cells, but not normal neural stem cells, were shown to express HDGF to directly induce tumour angiogenesis (33). Compared to wild-type hepatocellular carcinoma cells, tumour growth of their clone which had downregulated HDGF in vivo was also suppressed by inhibiting tumour angiogenesis rather than cell growth (34). While VEGF overexpression in NSCLC patients has been associated with a poor prognosis (23), no significant association has been found between the microvascular density in lesions and VEGF-A level in the blood of patients with advanced NSCLC (35). In addition to these reports, our findings show obvious evidence regarding the direct involvement of HDGF in human NSCLC cells and enhancement of VEGF-dependent angiogenesis by HDGF.

We performed serum-free culture with A549, Lu99 and EBC-1 cells and found that only EBC-1 cells could adapt to the culture. Consequently, cell death and HDGF mRNA expression in EBC-1 cells were little influenced regardless of whether FBS was present or absent, but the possibility of alteration of the cell condition in the serum-free culture
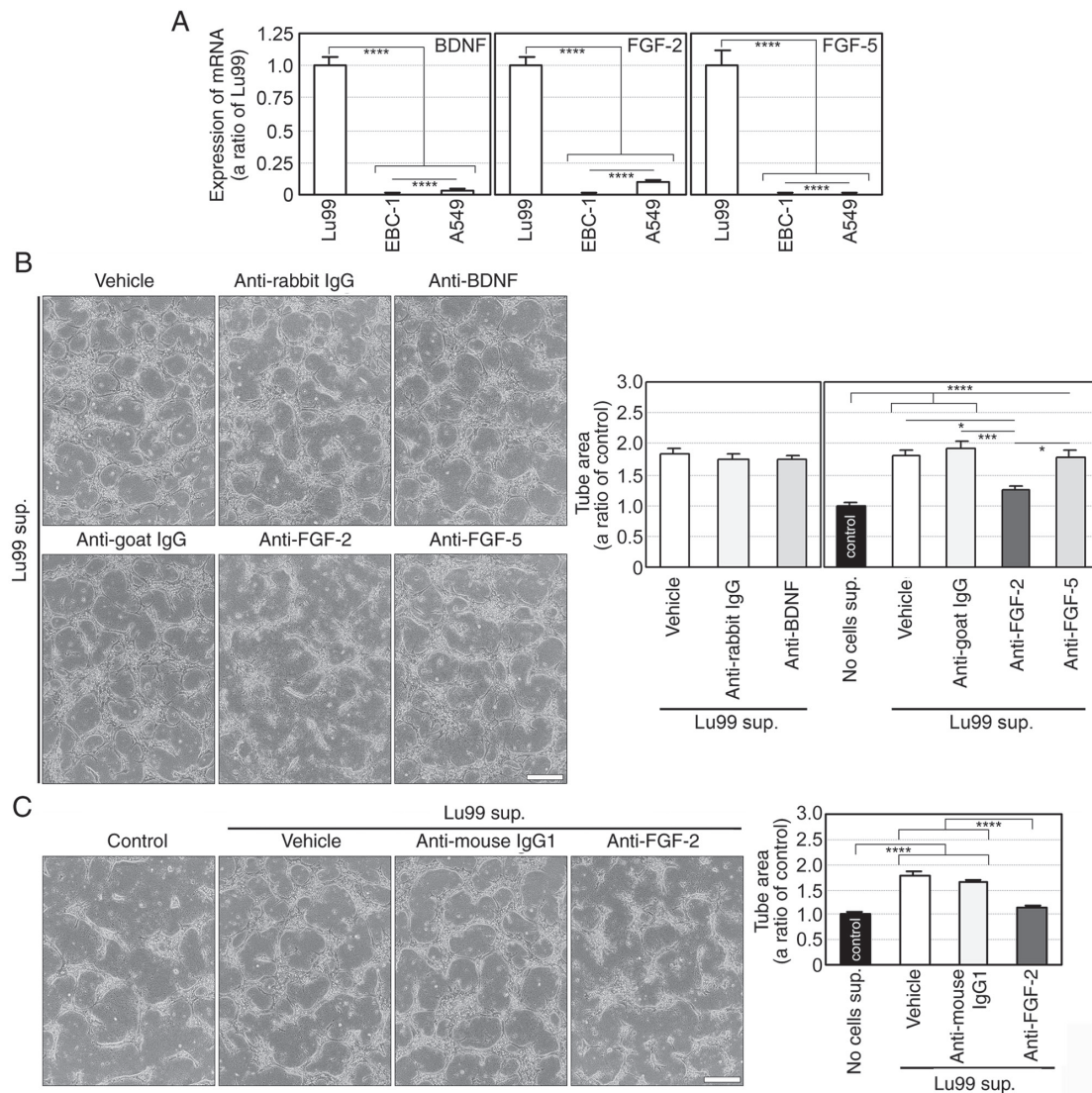
Figure 9. FGF-2 regulates HDGF- and VEGF-independent tube formation induced by the Lu99 supernatant (sup.). (A) mRNA expressions of BDNF, FGF-2 and FGF-5 in human NSCLC cells. Total RNA was isolated from Lu99, EBC-1 and A549 cells incubated with 10% FBS for 24 h, and then synthesis of first-strand cDNA and PCR was performed. Each expression level of BDNF, FGF-2 and FGF-5 mRNAs was normalised to the corresponding levels of 18S-rRNA as an internal control. ****P<0.001. (B) FGF-2, but not BDNF and FGF-5, is involved in Lu99 supernatant-induced tube formation. HUVECs sandwiched between two layers of collagen were incubated with tube-induction medium alone and that together with the rabbit polyclonal anti-IgG (10 µg/ml), the anti-BDNF, the goat polyclonal anti-IgG (10 µg/ml), the anti-FGF-2 or the anti-FGF-5 antibody, in which Lu99 supernatants were stratified, for 24 h. *P<0.05, ***P<0.005 and ****P<0.001. (C) FGF-2 in Lu99 supernatant induces HDGF- and VEGF-independent tube formation. HUVECs sandwiched between two layers of collagen were incubated with tube-induction medium alone and that together with the mouse monoclonal anti-IgG1 (10 µg/ml) or the anti-FGF-2 antibody, in which Lu99 supernatants were stratified, for 24 h. ****P<0.001. Each assay was performed in three independent experiments and representative images are shown. Data represent the means ± SEMs of three independent experiments. Statistically significant differences were determined by using one-way factorial ANOVA-Tukey's test. Scale bar, 100 µm. FGF-2, fibroblast growth factor-2; HDGF, hepatoma-derived growth factor; VEGF, vascular endothelial growth factor; BDNF, brain-derived neutrophic factor; FGF-2, fibroblast growth factor-2; FGF-5, fibroblast growth factor-5; HUVECs, human umbilical vein endothelial cells.

cannot be completely excluded. In addition, it was extremely difficult to confirm whether VEGF and HDGF function as angiogenic factors in A549 and Lu99 cells, as these cell lines could not adapt to the serum-free culture. Thus, we established a novel 3D culture method, which enabled culture supernatant, containing high concentrations of humoral factors derived from NSCLC cells, to be utilised without FBS condensation and cell contamination. By using the novel 3D culture method, we clarified that the Lu99 supernatant induced HDGF- and VEGF-independent tube formation and that FGF-2 regulated Lu99 supernatant-induced tube formation. FGF-2, also known as basic FGF, belongs to the FGF family which consists of

23 FGF heparin-binding polypeptides. FGF-2 is physiologically and pathologically an important regulator of cell growth, survival and differentiation such as development, tumourigenesis and angiogenesis (36). FGF-2 overexpression in operable NSCLC patients was found to be a prognostic indicator of poor survival (23,37,38), whereas stromal FGF-2 in patients with NSCLC receiving postoperative radiotherapy was found to be a positive prognostic factor for survival (39). Recently, a humanised anti-FGF-2 antibody produced by Wang *et al* was reported to reduce tumour growth of a NSCLC cell line (NCI-H460) and microvessel density in nude mice (40). The implication of FGF-2 for prognosis in NSCLC was
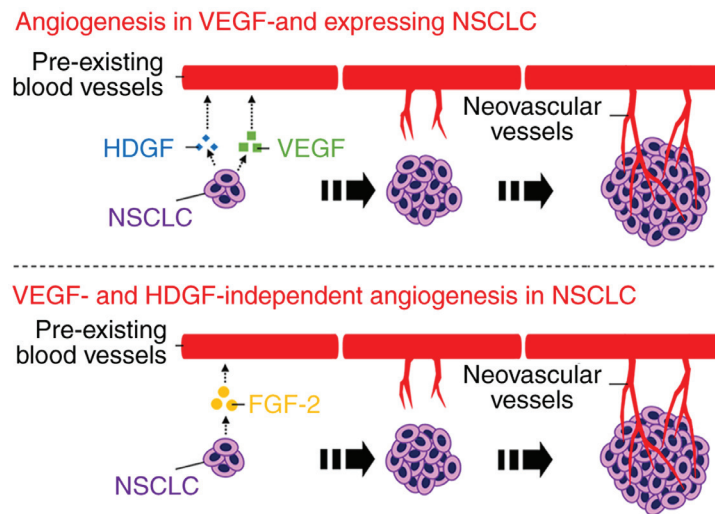
Figure 10. Schematic representation of angiogenic factors in NSCLC cells. HDGF enhances VEGF-dependent angiogenesis in VEGF-expressing NSCLC cells. FGF-2 induces VEGF-independent angiogenesis in VEGF-downregulated NSCLC cells. NSCLC, non-small cell lung cancer; HDGF, hepatoma-derived growth factor; VEGF, vascular endothelial growth factor; FGF-2, fibroblast growth factor-2.

controversial in these reports; however, based on these reports and our present study, FGF-2 overexpression in NSCLC cells is thought to induce tumour angiogenesis.

To determine the involvement of FGF-2 in Lu99 supernatant-induced tube formation, we transfected Lu99 cells with FGF-2 siRNA (siFGF-2). siFGF-2 did abrogate expression of FGF-2 (18 kDa) and its splicing variants (22, 22.5 and 24 kDa) in Lu99 cell lysate (Fig. S6A). It has been shown that FGF-2 proteins including the variants are lacking secretory signal peptide (41). The variants have both N- and C-terminal nuclear localisation signals (NLSs), but 18 kDa FGF-2 has only C-terminal NLS, and translocation of FGF-2 into the nucleus requires both NLSs, which means transportation of the splicing variants, but not 18 kDa FGF-2, into the nucleus (42). Intriguingly, FGF-2 in the Lu99 supernatant did not remain monomeric but instead formed oligomers, and their molecular weights differed from those of rhFGF-2 dimers and oligomers; siFGF-2 did not suppress FGF-2 secretion in the Lu99 supernatant (Fig. S6B). In addition to phosphoinositol 4,5-bisphosphate-dependent FGF-2 oligomerisation concomitant with membrane insertion (41,43), disassembly of membrane-inserted FGF-2 oligomers at the outer leaflet, mediated by cell-surface heparan sulphates, was recently reported (44). Type I collagen is also known to function as a FGF-2 reservoir (45). We therefore speculated that FGF-2 bound to heparan sulphates on the surface of Lu99 cells was retained after FGF-2 knockdown in Lu99 cells and that the residual FGF-2 was gradually transported to the extracellular space with the peptide chains of the heparan sulphates partially bound and then complexed with collagen in 3D culture. In fact, we tried to measure the FGF-2 concentration in Lu99 supernatant using the Human bFGF ELISA kit (RayBiotech, Inc.), but the kit, in which the anti-FGF-2 antibodies recognise rhFGF-2 monomer produced by *Escherichia coli*, failed to detect FGF-2 in the Lu99 supernatant. These results posed an issue that accurate measurements for FGF-2 of patients with NSCLC by ELISA need the anti-FGF-2 antibody to recognise not only FGF-2 monomer but also its oligomer. We also found

no involvement of FGF-2 in Lu99 cell proliferation *in vitro*, but further studies are needed to confirm whether FGF-2 inhibition by its neutralising antibodies and multi-tyrosine kinase inhibitors targeting FGF receptors suppresses tumour growth of NSCLC cells including A549 cells, in which serum-free culture could not be adapted and FGF-2 expression was extremely lower than in Lu99 cells, through *in vivo* assays to test the anti-angiogenic effect. Furthermore, future studies are needed to develop the experimental system for immunostaining of our 3D cultures to further evaluate the findings in the present study.

In conclusion, we demonstrated for the first time that HDGF enhances VEGF-dependent angiogenesis and that FGF-2 is a VEGF-independent angiogenic factor in human NSCLC cells. We hope that anti-angiogenic-antibody therapy targeting HDGF or FGF-2 can provide a novel treatment option for patients with NSCLC resistant to bevacizumab and ramucirumab.

Availability of data and materials

The data that support the findings of this study are available from the corresponding author upon reasonable request.

Authors' contributions

RE proposed the study, conducted the experiments and analysed the data. RE and IW designed the experiments and edited

the manuscript. Both authors read and approved the final manuscript and agree to be accountable for all aspects of the research in ensuring that the accuracy or integrity of any part of the work are appropriately investigated and resolved.

Ethics approval and consent to participate

Not applicable.

Patient consent for publication

Not applicable.

Competing interests

The authors declare that they have no competing interests.

References

1. Inoue M, Sawada N, Matsuda T, Iwasaki M, Sasazuki S, Shimazu T, Shibuya K and Tsugane S: Attributable causes of cancer in Japan in 2005-systematic assessment to estimate current burden of cancer attributable to known preventable risk factors in Japan. Ann Oncol 23: 1362-1369, 2012.
2. Siegel RL, Miller KD and Jemal A: Cancer statistics, 2016. CA Cancer J Clin 66: 7-30, 2016.
3. Villaruz LC and Socinski MA: The role of anti-angiogenesis in non-small-cell lung cancer: An update. Curr Oncol Rep 17: 26, 2015.
4. Hanahan D and Folkman J: Patterns and emerging mechanisms of the angiogenic switch during tumorigenesis. Cell 86: 353-364, 1996.
5. Dvorak HF: Vascular permeability factor/vascular endothelial growth factor: A critical cytokine in tumor angiogenesis and a potential target for diagnosis and therapy. J Clin Oncol 20: 4368-4380, 2002.
6. Ebos JM and Kerbel RS: Antiangiogenic therapy: Impact on invasion, disease progression, and metastasis. Nat Rev Clin Oncol 8: 210-221, 2011.
7. Yoh K, Hosomi Y, Kasahara K, Yamada K, Takahashi T, Yamamoto N, Nishio M, Ohe Y, Koue T, Nakamura T, et al: A randomized, double-blind, phase II study of ramucirumab plus docetaxel vs placebo plus docetaxel in Japanese patients with stage IV non-small cell lung cancer after disease progression on platinum-based therapy. Lung Cancer 99: 186-193, 2016.
8. Eguchi R, Nakano T and Wakabayashi I: Progranulin and granulin-like protein as novel VEGF-independent angiogenic factors derived from human mesothelioma cells. Oncogene 36: 714-722, 2017.
9. Livak KJ and Schmittgen TD: Analysis of relative gene expression data using real-time quantitative PCR and the 2(-Delta Delta C(T)) method. Methods 25: 402-408, 2001.
10. Ung TH, Madsen HJ, Hellwinkel JE, Lencioni AM and Graner MW: Exosome proteomics reveals transcriptional regulator proteins with potential to mediate downstream pathways. Cancer Sci 105: 1384-1392, 2014.
11. Bosque A, Dietz L, Gallego-Lleyda A, Sanclemente M, Iturralde M, Naval J, Alava MA, Martínez-Lostao L, Thierse HJ and Anel A: Comparative proteomics of exosomes secreted by tumoral Jurkat T cells and normal human T cell blasts unravels a potential tumorigenic role for valosin-containing protein. Oncotarget 7: 29287-29305, 2016.
12. Keeley EC, Mehrad B and Strieter RM: CXC chemokines in cancer angiogenesis and metastases. Adv Cancer Res 106: 91-111, 2010.
13. Chesney JA and Mitchell RA: 25 Years On: A retrospective on migration inhibitory factor in tumor angiogenesis. Mol Med 21 (Suppl 1): S19-S24, 2015.
14. Thijssen VL and Griffioen AW: Galectin-1 and -9 in angio-genesis: A sweet couple. Glycobiology 24: 915-920, 2014.
15. Kadomatsu K, Bencsik P, Gorbe A, Csonka C, Sakamoto K, Kishida S and Ferdinandy P: Therapeutic potential of midkine in cardiovascular disease. Br J Pharmacol 171: 936-944, 2014.
16. Palma G, Barbieri A, Bimonte S, Palla M, Zappavigna S, Caraglia M, Ascierto PA, Ciliberto G and Arra C: Interleukin 18: Friend or foe in cancer. Biochim Biophys Acta 1836: 296-303. 2013.
17. Funasaka T, Raz A and Nangia-Makker P: Galectin-3 in angio-genesis and metastasis. Glycobiology 24: 886-891, 2014.
18. Bao C, Wang J, Ma W, Wang X and Cheng Y: HDGF: A novel jack-of-all-trades in cancer. Future Oncol 10: 2675-2685, 2014.
19. Dai J, Peng L, Fan K, Wang H, Wei R, Ji G, Cai J, Lu B, Li B, Zhang D, et al: Osteopontin induces angiogenesis through activation of PI3K/AKT and ERK1/2 in endothelial cells. Oncogene 28: 3412-3422, 2009.
20. Ramazani Y, Knops N, Elmonem MA, Nguyen TQ, Arcolino FO, van den Heuvel L, Levtchenko E, Kuypers D and Goldschmeding R: Connective tissue growth factor (CTGF) from basics to clinics. Matrix Biol 68-69: 44-66, 2018.
21. He Z and Bateman A: Progranulin (granulin-epithelin precursor, PC-cell-derived growth factor, acrogranin) mediates tissue repair and tumorigenesis. J Mol Med (Berl) 81: 600-612, 2003.
22. Kermani P and Hempstead B: Brain-derived neurotrophic factor: A newly described mediator of angiogenesis. Trends Cardiovasc Med 17: 140-143, 2007.
23. Farhat FS, Tfayli A, Fakhruddin N, Mahfouz R, Otrock ZK, Alameddine RS, Awada AH and Shamseddine A: Expression, prognostic and predictive impact of VEGF and bFGF in non-small cell lung cancer. Crit Rev Oncol Hematol 84: 149-160, 2012.
24. Ghassemi S, Vejdovszky K, Sahin E, Ratzinger L, Schelch K, Mohr T, Peter-Vorosmarty B, Brankovic J, Lackner A, Leopoldi A, et al: FGF5 is expressed in melanoma and enhances malignancy in vitro and in vivo. Oncotarget 8: 87750-87762, 2017.
25. Nakamura H, Kambe H, Egawa T, Kimura Y, Ito H, Hayashi E, Yamamoto H, Sato J and Kishimoto S: Partial purification and characterization of human hepatoma-derived growth factor. Clin Chim Acta 183: 273-284, 1989.
26. Everett AD, Narron JV, Stoops T, Nakamura H and Tucker A: Hepatoma-derived growth factor is a pulmonary endothelial cell-expressed angiogenic factor. Am J Physiol Lung Cell Mol Physiol 286: L1194-L1201, 2004.
27. Ren H, Chu Z and Mao L: Antibodies targeting hepatoma-derived growth factor as a novel strategy in treating lung cancer. Mol Cancer Ther 8: 1106-1112, 2009.
28. Ren H, Tang X, Lee JJ, Feng L, Everett AD, Hong WK, Khuri FR and Mao L: Expression of hepatoma-derived growth factor is a strong prognostic predictor for patients with early-stage non-small-cell lung cancer. J Clin Oncol 22: 3230-3237, 2004.
29. Iwasaki T, Nakagawa K, Nakamura H, Takada Y, Matsui K and Kawahara K: Hepatoma-derived growth factor as a prognostic marker in completely resected non-small-cell lung cancer. Oncol Rep 13: 1075-1080, 2005.
30. Zhao WY, Wang Y, An ZJ, Shi CG, Zhu GA, Wang B, Lu MY, Pan CK and Chen P: Downregulation of miR-497 promotes tumor growth and angiogenesis by targeting HDGF in non-small cell lung cancer. Biochem Biophys Res Commun 435: 466-471, 2013.
31. Ke Y, Zhao W, Xiong J and Cao R: Downregulation of miR-16 promotes growth and motility by targeting HDGF in non-small cell lung cancer cells. FEBS Lett 587: 3153-3157, 2013.
32. Guo H, Li W, Zheng T and Liu Z: MiR-195 targets HDGF to inhibit proliferation and invasion of NSCLC cells. Tumour Biol 35: 8861-8866, 2014.
33. Thirant C, Galan-Moya EM, Dubois LG, Pinte S, Chafey P, Broussard C, Varlet P, Devaux B, Soncin F, Gavard J, et al: Differential proteomic analysis of human glioblastoma and neural stem cells reveals HDGF as a novel angiogenic secreted factor. Stem Cells 30: 845-853, 2012.
34. Enomoto H, Nakamura H, Liu W, Iwata Y, Nishikawa H, Takata R, Yoh K, Hasegawa K, Ishii A, Takashima T, et al: Down-regulation of HDGF inhibits the growth of hepatocellular carcinoma cells in vitro and in vivo. Anticancer Res 35: 6475-6479, 2015.
35. Bacic I, Karlo R, Zadro AS, Zadro Z, Skitarelic N and Antabak A: Tumor angiogenesis as an important prognostic factor in advanced non-small cell lung cancer (Stage IIIA). Oncol Lett 15: 2335-2339, 2018.
36. Akl MR, Nagpal P, Ayoub NM, Tai B, Prabhu SA, Capac CM, Gliksman M, Goy A and Suh KS: Molecular and clinical significance of fibroblast growth factor 2 (FGF2 /bFGF) in malignancies of solid and hematological cancers for personalized therapies. Oncotarget 7: 44735-44762, 2016.

37. Hu M, Hu Y, He J and Li B: Prognostic value of basic fibroblast growth factor (bFGF) in lung cancer: A systematic review with meta-analysis. PLoS One 11: e0147374, 2016.

38. Hu MM, Hu Y, Gao GK, Han Y, Shi GL and Li BL: Basic fibroblast growth factor shows prognostic impact on survival in operable non-small cell lung cancer patients. Thorac Cancer 6: 450-457, 2015.

39. Andersen S, Donnem T, Al-Saad S, Al-Shibli K, Busund LT and Bremnes RM: Angiogenic markers show high prognostic impact on survival in marginally operable non-small cell lung cancer patients treated with adjuvant radiotherapy. J Thorac Oncol 4: 463-471, 2009.

40. Wang S, Qin Y, Wang Z, Xiang J, Zhang Y, Xu M, Li B, Xia Y, Zhang P and Wang H: Construction of a human monoclonal antibody against bFGF for suppression of NSCLC. J Cancer 9: 2003-2011, 2018.

41. La Venuta G, Zeitler M, Steringer JP, Muller HM and Nickel W: The startling properties of fibroblast growth factor 2: How to exit mammalian cells without a signal peptide at hand. J Biol Chem 290: 27015-27020, 2015.

42. Sorensen V, Nilsen T and Wiedlocha A: Functional diversity of FGF-2 isoforms by intracellular sorting. Bioessays 28: 504-514, 2006.

43. Muller HM, Steringer JP, Wegehingel S, Bleicken S, Munster M, Dimou E, Unger S, Weidmann G, Andreas H, Garcia-Saez AJ, et al: Formation of disulfide bridges drives oligomerization, membrane pore formation, and translocation of fibroblast growth factor 2 to cell surfaces. J Biol Chem 290: 8925-8937, 2015.

44. Dimou E, Cosentino K, Platonova E, Ros U, Sadeghi M, Kashyap P, Katsinelos T, Wegehingel S, Noe F, Garcia-Saez AJ, et al: Single event visualization of unconventional secretion of FGF2. J Cell Biol 218: 683-699, 2019.

45. Kanematsu A, Marui A, Yamamoto S, Ozeki M, Hirano Y, Yamamoto M, Ogawa O, Komeda M and Tabata Y: Type I collagen can function as a reservoir of basic fibroblast growth factor. J Control Release 99: 281-292, 2004.